

**Introduction:** Carbonados are porous polycrystalline (with crystal sizes up to 100  $\mu\text{m}$ ) diamonds [1]. Carbonado is found only in alluvial deposits in Bahia, Brazil and in the Central African Republic (CAR). Alluvial deposit host is 1.5 Ga while the carbonados are between 2.6 – 3.8 Ga [2]. The process of fusing the carbonado microcrystals together is not fully understood, partly due to fact that the origin of these carbonado is not known.

**Models of origin:** Several modes of origins are proposed for carbonado [3]. First, a crustal origin. Carbonados have a light carbon and helium isotopic signature [4,5]. They contain an enrichment of the light rare-earth elements (REE) [4,6]. Carbonados have tightly trapped atmospheric noble gases [7] and contain an evidence of high He content despite the carbonado expected depletion of He at mantle temperatures [8]. Carbonados have high porosity incompatible with high pressure mantle conditions [9].

Second, a mantle origin is proposed based on similar REE pattern to kimberlites [10,11]. The presence of nitrogen platelet (by IR spectra) indicates high temperature origin [10,12] and syngenetic inclusions of rutile, ilmenite, and magnetite indicates high pressure and high temperature conditions consistent with mantle origin as well [13].

Third, it is proposed that carbonado diamonds are a result of early impacts into crustal rocks. This is indicated by the rare and controversial occurrence of high pressure diamond polymorph, lonsdaleite, frequently found in diamonds from meteorite impact sites [14], and by observation of planar deformation features, possibly indicating shock events [15].

Finally, it is suggested that carbonados have an extraterrestrial origin, as indicated by a long term annealing based on observation of a zero-phonon line, attributed to paired nitrogen atoms in association with a vacancy [9].

**Previous magnetic work:** Collinson [16] carried out a magnetic properties study and his results are summarized. NRM intensity (natural remanent magnetization) ( $1\text{-}10 \cdot 10^{-5} \text{ Am}^2\text{kg}^{-1}$ ) is stable with very small decrease ( $\sim 10\%$ ) after demagnetization to 100 mT. The NRM directions show a steady migration to stable primary endpoints with irregular intensity decay curves. When measured in high magnetic field gradient as a function of temperature, carbonados showed a low magnetic discontinuity at 120 – 160 C. An initial magnetic susceptibility was in a range  $5 \cdot 10^{-8} \text{ m}^3\text{kg}^{-1}$ .

During acquisition of an isothermal remanent magnetization (IRM) there is no indication of saturation being reached at 800mT applied field.  $J_s/\text{NRM}$  ratio is between 10 – 100 as oppose to a typical range of terrestrial material which is in between 100-1000 [17].

**Material and method:** We obtained 20 samples of carbonados from the CAR. They are of variable sizes, colors and morphology. Samples show pores of varying number and size which decrease in quantity where the surface is glassy smooth. All samples were cleaned with the ultrasound cleaner before any procedures started. NRM and Saturation Isothermal Remanent Magnetization (SIRM) of carbonados were measured with the Superconducting Rock Magnetometer (SRM). Hysteresis properties of strongly magnetic samples were measured with the vibrating sample magnetometer (VSM). Magnetic fields up to 2 T were used. Surfaces of all samples were characterized by optical microscopy and Scanning Electron Microscopy. Samples with a detectable magnetic signature were cleaned in a mixture of 1 part 50% HF acid and 1 part 6N solution of nitric acid for 24 hours to remove surface contamination. Than they were washed in 6N solution of hydrochloric acid renewing it every 3 days. During the acid change the samples were cleaned ultrasonically as well. Mass and SIRM were measured after 14, 46, 64 days. Even after 64 days samples still kept reacting to the HCL as indicated by the yellow coloration of the acid towards the end of the 3 day period, when the acid was due to change. However, the magnetic signature dropped significantly. At the end of the acid treatment samples were characterized by SEM microscopy.

**Magnetic Results:** Table 1 summarizes the magnetic characteristic before acid treatment.

sample	weight [mg]	NRM [ $\text{Am}^2\text{kg}^{-1}$ ]	SIRM [ $\text{Am}^2\text{kg}^{-1}$ ]	REM NRM/SIRM	Hc [Tesla]	$J_s$ [ $\text{Am}^2\text{kg}^{-1}$ ]
D1	238.2	0.000004	0.000101	0.0431	0.02	0.0002
D2	143.1	0.000011	0.000107	0.0991		0.0002
D3	233.3	0.000005	0.000324	0.0086		
D5	214.6	0.000005	0.000039	0.1367		0.0001
D4	160.5	0.000099	0.000393	0.2522	0.0015	0.0057
D6	170.1	0.000008	0.001067	0.0075		
D7	255.0	0.000004	0.000352	0.0109		
D8	197.7	0.000007	0.000020	0.3304		
D9	215.6	0.000004	0.000159	0.0222	0.05	0.0004
D10	175.1	0.000006	0.001067	0.0061		
D11	5123.4	0.000004	0.005607	0.0007	0.031	0.0105
D12	3456.8	0.000003	0.000200	0.0137	0.10	0.0002
D13	618.8	0.000002	0.000230	0.0087		
D14	467.4	0.000002	0.000736	0.0031	0.1	0.0015
D15	410.2	0.000049	0.000542	0.0911	0.0005	0.012
D16	616.8	0.000002	0.000154	0.0143		
D17	519.9	0.000002	0.000104	0.0227		
D18	297.9	0.000003	0.000011	0.2940		
D19	405.0	0.000002	0.000151	0.0143		
D20	394.8	0.000020	0.000183	0.1080		0.0003

Table 1:

NRM values ranged between  $0.1\text{-}10 \cdot 10^{-5} \text{ Am}^2\text{kg}^{-1}$  which is consistent with the measurements by [16]

who reports the same range of NRM values. Saturation magnetization ranged in between  $1.0\text{-}500 \cdot 10^{-5} \text{ Am}^2\text{kg}^{-1}$  and REM values between 0.001-0.3. The hysteresis parameters were measured only on a limited number of samples, due to lower sensitivity of VSM. Loops were often constricted, indicating two magnetic components with different coercivities. One loop (sample D15) resembled native iron based on a large saturation field. All of the samples showed a diamagnetic component ( $-2 \cdot 10^{-2} \text{ A m}^2\text{kg}^{-1}$ ), due to the diamond matrix.

Acid cleaning resulted in loss of both saturation remanence (Fig. 1) and mass (Fig. 2) of the samples.

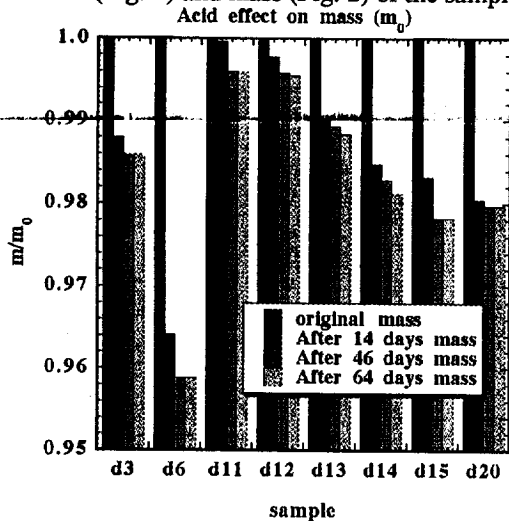


Fig. 1:

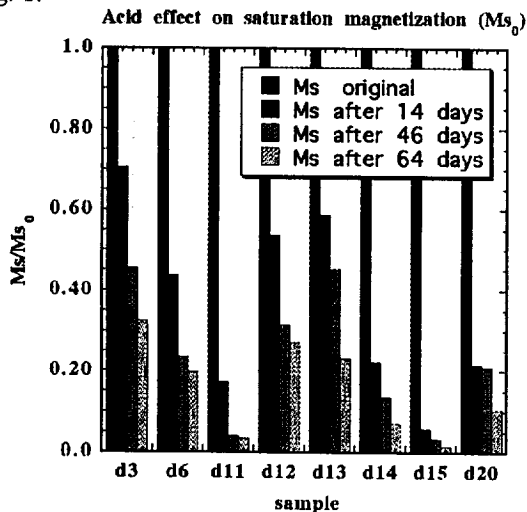


Fig. 2:

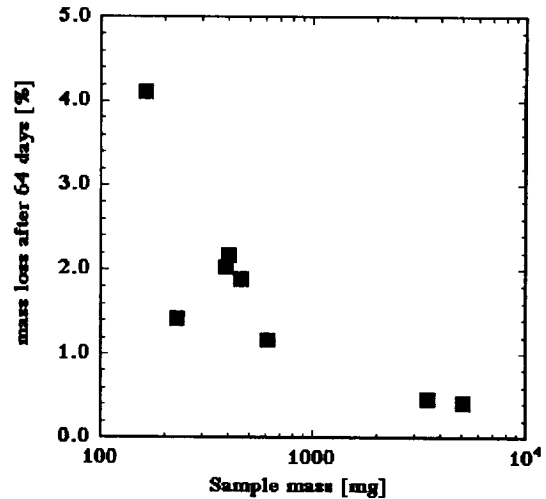


Fig. 3:

A much greater percent of the magnetic signal was lost compared with mass loss. Amount of mass loss from the sample was dependent on size (Fig.3).

This is probably due to increase of the surface area vs. volume with decreasing carbonado size. Thus the acid desolves smaller grains more efficiently than large ones. However, the magnetization loss is essentially independent on the size of the original sample (Fig 4).

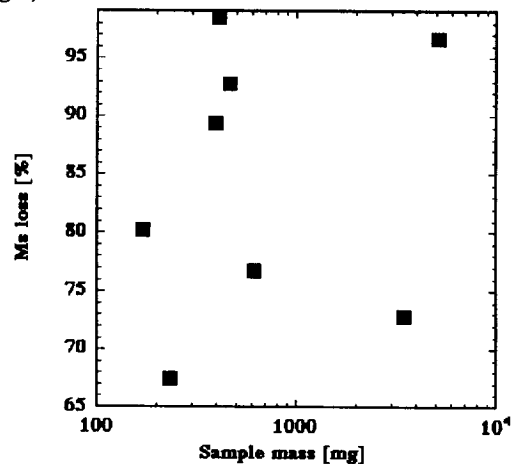


Fig. 4:

This independence in size and large amount of magnetization lost indicate that most of the magnetic material is concentrated on the carbonado surface.

Because magnetism of Carbonado comes from the surface, indicating contemporary formation of both the surface and magnetic carriers and/or some kind of later chemical contamination, the interior of carbonado must be relatively free of magnetic phases.

**References:** [1] Trued, L. F. et al. (1971) *Am Miner.*, 59, 1252-1268. [2] Ozima, M. et al. (1997) *GCA*, 61, 369-376. [3] Haggerty, S. E. (1999) *Science*, 285, 851-860. [4] Kamioka, H. et al. (1996) *Geochem. J.*, 30, 189-194. [5] Burgess, R. et al. (1998) *Chem. Geol.* 146, 205-217. [6]

Shibata, K. et al. (1993) *Min. Mag.*, 57, 607-611. [7]  
Ozima, M. et al. (1991) *Nature*, 351, 472-474. [8] Zashu, S.  
et al. (1995) *GCA*, 59, 1321-1328. [9] Haggerty, S. E.  
(1998) *Proc 5th NIRIM Int. Symp. Adv. Mat.*, 39-42. [10]  
Kagi, H. et al. (1994) *GCA*, 58, 2629-2638. [11] Gorshkov,  
A. I. et al. (1997) *Geol. Ore Dep.*, 39, 229-236. [12]  
Shelkov, D. et al. (1997) *Geol. Geof.*, 38, 315-322. [13]  
Gorshkov, A. I. et al. (1996) *Geol. Ore Dep.*, 38, 114-119.  
[14] Smith, J. V. et al. (1985) *Geology*, 13, 342-343.  
[15] De, S. et al. (1999) *EPSL*, 164, 421-433. [16] Collin-  
son, D. W. (1998) *EPSL*, 161, 179-188. [17] Wasilewski, P.  
J. (1977) *PEPI*, 15, 349-362.